Research Square

Preprints are preliminary reports that have not undergone peer review.
They should not be considered conclusive, used to inform clinical practice,
or referenced by the media as validated information.

Pseudomonas fluorescens driven Biocatalytic Depolymerization of Polyethylene Terephthalate (PET) and Polystyrene (PS) Matrices: Implications for Sustainable Plastic Waste Valorization

Niketha Manoj
National Institute of Technology Calicut
Manoj A
National Institute of Technology Calicut
Bhaskar S
National Institute of Technology Calicut
Damodharan P
National Institute of Technology Calicut
Alok Anthappan Martin
National Institute of Technology Calicut
Shabina Ashraf
shabinaashraf@nitc.ac.in
National Institute of Technology Calicut

Research Article

Keywords: Plastic biodegradation, Pseudomonas fluorescens, Polystyrene, Polyethylene terephthalate, UV pretreatment, Soil

Posted Date: July 5th, 2026

DOI: https://doi.org/10.21203/rs.3.rs-10041116/v1

License: This work is licensed under a Creative Commons Attribution 4.0 International License.
Read Full License

Additional Declarations: No competing interests reported.

Version of Record: A version of this preprint was published at Discover Sustainability on October 5th, 2026. See the published version at https://doi.org/10.1007/s43621-026-04894-z.

Abstract

The escalating environmental threat caused by the accumulation of recalcitrant synthetic plastics necessitates the development of effective bioremediation strategies. This study investigates the biodegradation potential of *Pseudomonas fluorescens* on two distinct substrates: two-dimensional PET (Poly Ethylene Terephthalate) sheets and three-dimensional PS (Poly Styrene) blocks. The influence of UV pretreatment on microbial degradation efficiency was also evaluated. A sequential batch culture method was employed for four weeks at 30°C. Degradation was monitored via gravimetric analysis, Scanning Electron Microscopy (SEM) and Fourier-Transform Infrared Spectroscopy (FTIR). UV pretreatment significantly enhanced biodegradation efficiencies, resulting in higher percentage weight losses by the fourth week, for both PET (7.11% for UV pretreated vs. 5.33% for untreated samples) and PS (41.42% for UV pretreated vs. 32.5% for untreated samples). SEM analysis revealed progressive structural deterioration; PET samples displayed severe fracturing and flaking, while PS blocks exhibited major hollow cavity formations in the structure causing the loss of structural integrity. The PET samples also showed significant changes in the FTIR peaks in the third and fourth weeks in the wave number regions 1000 cm^{-1} to 1700 cm^{-1}, indicating the loss of integrity in the polymer structure, leading to significant fragmentation. FTIR of PS suggested that the accelerated onset of biodegradation was driven by early and prominent formation of hydroxy/hydroperoxide groups evident from the broadening of the peak at 3400 cm^{-1}. This study suggests that *P. fluorescens* effectively destabilizes polymer integrity by inducing both surface erosion and molecular cleavage, highlighting its promise for sustainable plastic waste mitigation.

1. Introduction

As global population growth accelerates industrial expansion, our reliance on synthetic polymers has driven an unprecedented surge in plastic production [1]. Plastic resists biodegradation and remains in the ecosystem for centuries, progressively fragmenting into microplastics (MPs) and nano plastics that endanger wildlife and human health [2–4]. Traditional solid waste management approaches are inadequate because plastics are highly recalcitrant in landfills, causing physical, chemical and biological harm to ecosystem [5]. Although mechanical and chemical recycling methods are available, including incineration and recycling, they are retarded by significant drawbacks such as elevated energy demands, often leading to poor performance with mixed or contaminated plastic feedstock, considerable costs and risk of secondary pollution like emission of toxic byproducts [6, 7]. While the durability of plastics promotes their usage, the persistent accumulation across all ecosystems in the long term is dangerous [8–10].

In the terrestrial ecosystem, soil health is under mounting pressure from plastic particulates, which profoundly disrupt it by altering soil physiochemical properties and microbial communities [11]. Microscopic fragments of plastics present in the soil, termed MPs, enter via diverse routes, including fertilizers from biowaste processing plants and breakdown of discarded material such as plastic mulch films [12, 13]. Moreover, a multitude of MPs fragments and fibers found in sewage and sludge pose a

risk to the ecosystem and human health. Reports document plastic particulate accumulation across the globe, particularly at the shores and coastlines [14]. Infrequent aerator cleaning can also drive higher MP contamination in the drinking water system [15]. In a recent spatial assessment of a 0.92 km^2 coast in Tamil Nadu, researchers found an abundance of filamentous and fragmented MPs predominantly concentrated in wet sand. SEM and FTIR analysis identified majority of MPs as PS, Polypropylene (PP), Polyethylene (PE) and Poly Amide (PA) [16]. In Bihar, the majority of plastic contamination in agricultural soil is influenced by plastic mulching, and poor management of PE-based mulch films. The study was conducted across 22 sites in 6 districts where mean MPs ranged from 150–1460 particles kg^{-1} soil [17]. MPs were detected in paddy field soil samples from Goa and Udupi, with Goa showing the higher overall contamination [18].

The behavior of PE majorly depends on physiochemical properties like density and crystallinity [19]. Studies from Eastern India show that PP and PE fibers and fragments pile up mainly in surface soil, while the finer particles move deeper in the vadose zone. Using Microplastic Pollution Load Index (MPPLI), researchers located pollution hotspots and linked these contaminants to the changes occurring in the soil organic matter and electrical conductivity [20]. The accumulation of plastics in the vadose zone soil layers poses a threat to the food chain [21, 22]. As plant roots interact with different types and concentrations of plastic particulates, understanding plastic biodegradation is important for waste management and the development of sustainable strategies.

Microbial communities were recently investigated to understand the biodegradation potential of MPs. In this regard, members of the genus *Pseudomonas*, which are ecologically widespread, possess a diverse metabolic capability enabling them to colonise a vast spectrum of ecological niches, including the complex interface of soil and rhizosphere [23]. *P. fluorescens* is not a single species but a member of highly adaptable strains, which are known for their ability to grow in impacted sites. It comprises eight distinct groups (including *P. fluorescens, P. gessardii, P. fragi, P. mandelii, P. koreensis, P. jessenii, P. corrugata* and *P. chlororaphis*), that occupy various ecological niches [24]. There are several studies reported on the implications of bacterial assisted biodegradation, such as *Priestia aryabhattai* VT 3.12, Bacillus *pumilus* VT 3.16 and *Bacillus pseudomycoides* VT 3.15, which facilitate enhanced PET degradation [25]. Notably, *Gordonia polyisoprenivorans* B253 can efficiently degrade PP and PS [26], whereas *Enterobacter hormaechei* has been identified as a potential agent capable of achieving significant mass reduction in PET [27]. However, most of these studies explore specific strains, whose availability in the vadose zone may be limited. Investigating plastic biodegradation using a readily available bacterial strain from the soil layers, which interacts with the rhizosphere, can provide a multi-faceted solution strategy where, the bacteria can degrade the plastics and simultaneously improve soil health. In this study, we investigate the biocatalytic ability of *P. fluorescens*, a plant growth promoting rhizobacterium (PGPR), which is also known to enhance nutrient availability and acts as a biocontrol agent.

The current research explores two distinct structural formats of plastic types, (1) two-dimensional (2D) PET sheets, which represent high surface area for microbial interaction, and (2) three-dimensional (3D)

PS blocks, which represent complex, high volume rigid matrices. Most of the plastic particulates on the soil surfaces are constantly exposed to UV-A and UV-B rays. To understand the role of UV exposure in plastic biodegradation, we have also considered the effects of UV pretreatment on PS and PET samples. The comparison of biodegradation on UV pretreated and untreated plastic samples is critical for understanding how photo oxidative weathering, a natural environmental process, alters polymer crystallinity and surface hydrophobicity. By evaluating these diverse physical states and pretreatment conditions, this research aims to provide a comprehensive framework for the sustainable valorization of plastic particulates.

2. Methodology

In this study, the bacterial strain *P. fluorescens* was obtained from the Microbial Type Culture Collection (MTCC) and Gene Bank, from CSIR- Institute of Microbial Technology, Chandigarh, India. The bacterial sample was cultured in the nutrient media. The cultures were kept in conditions that were carefully regulated, at a temperature of 30°C and a pH of 7 ± 0.2.

Two plastic types were used for the study; (1) PET sheets of areal size 1 cm^2 and (2) PS blocks of volume 1 cm^3. Plastic samples were surface sterilized by immersion in 70% isopropyl alcohol for 10 minutes, followed by thorough rinsing with sterile distilled water. The plastic samples considered for the UV treatment were placed under a UV source for 100 hours. All the samples were stored aseptically and protected from light until their introduction into the microbial cultures.

The biodegradation experiments were conducted by aseptically adding four samples each of UV pretreated and untreated samples of PET and PS to the culture flasks containing *P. fluorescens*. Abiotic control flasks without *P. fluorescens*, containing only the sterilized media, along with PET and PS samples, were also considered for comparison, which served as the control samples. The incubation time of *P. fluorescens* is approximately one week. The experimental conditions were controlled through weekly serial incubations in new culture media flasks for four weeks in a shaker incubator at 30℃ and 150 rpm. One sample of each PET and PS was withdrawn from the culture medium using forceps every week. The other samples are aseptically introduced into new culture medium flasks to assess further biodegradation. The weekly withdrawal process of samples for the four consecutive weeks is labelled as week-I, week-II, week-III, and week-IV, respectively. To remove the surface bacterial biomass of the isolated samples from the culture flasks, they were cleaned using 2% SDS solution [28], followed by extensive washing with 70% ethanol and sterile distilled water, to remove loosely attached cells and media residues. The samples are then dried at 50°C to a constant weight before further analysis [29]. To evaluate the microstructural alterations and chemical depolymerization characteristics of *P. fluorescens* during the four-week biodegradation, the samples were analyzed using SEM and FT-IR, in addition to gravimetric analysis.

3. Results and Discussions

3.1 Weight loss of PET and PS upon treatment with *P. fluorescens*

The gravimetric analysis evaluates the percentage weight loss for each sample. The percentage weight loss for each sample is evaluated using Eq. (1).

$$WL = \left(\frac{W_{initial} - W_{final}}{W_{initial}} \right) 100$$

1

where, *WL* is the degradation percentage evaluated based on, $W_{initial}$, which is the initial weight of the plastic sample before biodegradation, and W_{final}, the final weight of plastic sample after biodegradation.

The initial weight of the PET sheet (1 cm^2) was 0.09 gm, which remained consistent across all the samples. The initial weight of the PS block was 0.02 gm for the untreated sample, and for the UV pretreated samples, it was 0.014 gm. The percentages of weight loss reported in this study are evaluated using Eq. (1), as shown in Table 1. The UV pretreated PET sheet biodegraded to a final weight loss of 7.11% by week-IV, whereas, at the end of week-IV, the untreated PET sheet had a weight loss of only 5.33%, which is 1.78% less than that of UV pretreated sample. It could be observed from Table 1 that the untreated PET sample *WL* was similar to the *WL* of UV pretreated samples from the previous week, i.e., the *WL* of PET for UV pretreated samples in week-I, II, III are similar to the *WL* of untreated samples in week-II, III, IV, respectively. This indicates that the gravimetric biodegradation was approximately accelerated by one week's time due to UV pretreatment. This also suggests that in natural environments, the PET samples in the top layers of soil are exposed to UV rays, and the degradation timescales shorten as compared to those buried underneath.

Table 1
Biodegradation of PET and PS by *P. fluorescens*

Polymer	Sample	Week wise degradation (WL in %)			
		I	II	III	IV
PET sheet ($1cm^2$)	Untreated control	0	0	0	0
	UV treated control PET	0	0	0	0
	Untreated PET	0	1.22	3	**5.33**
	UV treated PET	1.11	3.33	5.44	**7.11**
PS block ($1cm^3$)	Untreated control	0	0	0	0
	UV treated control PS	0	0	0	0
	Untreated PS	1.5	7.5	15.5	**32.5**
	UV treated PS	2.85	7.85	25.57	**41.42**

Similarly, for the PS samples, from Table 1, the UV treated samples showed a degradation of 41.42% by the end of week-IV, whereas the untreated PS sample degradation, by the end of week-IV is 32.5%. The UV pretreated PS sample showed an additional 8.92% more degradation than the untreated sample. It could also be observed from Table 1 that, during the first two weeks, the UV pretreated samples showed only a slightly higher *WL* than the untreated samples, indicating that the early time degradation in UV pretreated and untreated samples remains similar. However, during weeks-III and IV, the *WL* of UV pretreated samples showed a sharp increase in *WL*. This indicates that, UV exposure affects the sample biodegradability in the long run, indicating that the top soil layers' PS samples might seem unaffected initially, in the longer durations are more susceptible to attack by *P. fluorescens*.

The data in Table 1 is graphically represented in Fig. 1. For PET sheet, we see from Fig. 1 that, the *WL* is consistently higher for UV pretreated sample from week-I, through the weeks- II, III and IV. For PS samples the *WL* did not significantly change during the first two-weeks. In week-III and IV, the degradation of UV treated PS block increases sharply, as compared to that of untreated samples. It could also be inferred from Fig. 1 that, the cumulative *WL* for PS block is significantly more that the PET sheet, indicating that the biodegradation by *P. fluorescens* is much faster in PS samples.

This higher weight loss in UV pretreated PET and PS samples could be due to the UV light triggering the breakdown of the polymeric backbone through a process called photolysis, making it easier for the sample material to degrade.

3.2 Surface morphological changes of PS and PET treated with *P. fluorescens*

The biodegraded samples were investigated by SEM, and micrographs of PET and PS samples are shown in Figs. 2 and 3, respectively, for both the untreated and UV pretreated scenarios.

SEM analysis of the PET sheets in Fig. 2(a), shows a continuous, non-porous surface for the control sample, which was placed in the sterilized media without bacteria. For the PET samples placed in the inoculum, localized curls and abrasions were observed by the end of week-II, as shown in Fig. 2(b). By the end of week-IV, these features evolved into prominent longitudinal cracks and visible surface flaking, evident from Fig. 2(c). The fragmentation of PET samples by the end of week-IV is evident from Fig. 2(c). These results were in concurrence with the PET degradation study in the marine environment, where similar observations were made [30]. The surfaces are now more amorphous than they were prior to bacterial treatment, similar to that observed in a study where *S. maltophilia BK1* and *Enterococcus sp. BK3* potentially degraded low density polyethylene [31].

The Fig. 2(d), (e), (f) show SEM images for UV pretreated samples, for control, week-II, and week-IV scenarios, respectively. We observed from the gravimetric analysis that the UV pretreated samples demonstrated a higher biodegradability as compared to that of the untreated samples. The control sample for UV pretreated PET shown in Fig. 2(d), is similar to the UV untreated sample shown in Fig. 2(a). The UV pretreated sample has displayed a weathered texture, with localized abrasions, grooves, pitting and striations, by the end of week-II, as shown in Fig. 2(e). By the end of week-IV, the UV pretreated PET sample shows a significant surface roughness and layer peeling, and even cracking, with significant morphological changes, as shown in Fig. 2(f). Fragments of the sample material adhering to the sample backbone could also be observed from Fig. 2(f), indicating the fragmentation of the material. The untreated PET sample shows a visibly higher fragmentation in the SEM image (Fig. 2c), as compared to the UV pretreated sample (Fig. 2(f)); which could be due to the higher number of fragments dissociating from the backbone of the PET for the UV pretreated sample. We can see from the untreated PET sample that (Fig. 2(b)), a large smooth groove is formed during week-II, followed by deepening of the groove and fragmentation by week-IV. For the UV pretreated PET sample, we see that multiple surface flaking incisions have formed by week-II (Fig. 2(e)), which develop into deep grooves with fragmented features. Although the SEM images could not clearly represent the biodegradation phenomena, this could be inferred from the gravimetric analysis shown in Table 1 and Fig. 1 for untreated and UV pretreated PET samples. Literature studies indicate that the cracks in PET biodegradation are expected to act as essential anchoring points for *P. fluorescens*, increasing the available surface area for colonization [32, 33]. The multiple incisions during week-II for UV retreated sample (Fig. 2(e)) indicate that more bacterial colonization could be supported, as compared to the untreated sample. Bacteriological action is also known to facilitate the surface for an increase in crack formation [34]. The morphological evidence confirms a synergistic degradation mechanism in which an initial UV pretreatment enhances bacterial breakdown of plastic.

The SEM micrographs of the PS blocks illustrate a clear progression of bacterial erosion for both the untreated and UV pretreated samples. The control sample shown in Fig. 3(a), displays a homogenous, smooth surface, indicating the absence of biodegradation and the absence of pits and grooves in the

material. The smooth, layered surfaces in Fig. 3(a) indicate the undisturbed integrity of the PS material. By the end of week-II, the signs of biodegradation appear as localized cavities, pits and microgrooves, with lateral dimensions of the irregular cavities measured at 75.838 µm, 82.562 µm and 105.825 µm, using image J software. Figure 3(c) shows that by the end of week-IV, the morphological surface degradation transitions into deep pits where the PS polymer has eroded from beneath the top surface, thereby indicating significant material loss, similar to the phenomena reported in the literature [28].

In the UV pretreated samples, the control sample shown in Fig. 3(d), exhibits microfractures from photooxidation phenomena. This indicates that PS can photodegrade even in the absence of bacteria, with irregular sized cavity formations, an unsystematic layer arrangement and a significant morphological change in PS surface is observed. The biodegradation at the end of week-II, as shown in Fig. 3(e) indicates that the morphological transition appears to be relatively smooth as compared to the untreated PS sample (in Fig. 3(b)). This could be due to biofragmentation, where the uneven top layers detach from the main structure due to the prior photooxidation, facilitating the biodegradation, which supports the gravimetric analysis from Table 1. In Fig. 3(f), we see a highly rugged, mulched topological feature indicating massive structural disintegration by the end of week-IV.

The distinct degradation patterns such as cavitation and pitting in PET versus delamination and hollowing phenomena in PS are a result of the polymers' physical densities. The porous nature of PS blocks allows for volumetric erosion, while the crystalline structure of PET sheets limits microbial activity to surface level etching. The progression from a smooth control to the degraded week-IV samples, visually validates the biodegradation occurring at the plastic biodegradation assisted by *P. fluorescens*.

3.3 FTIR analysis

To elucidate the mechanism of degradation of *P. fluorescens*, Attenuated Total Reflectance-FTIR (ATR-FTIR) spectra were measured for the control and four-week test samples. Significant spectral modifications were observed between wave numbers 4000 cm^{-1} and 500 cm^{-1}, reflecting dynamic changes in vibrational phenomena of the polymers during biodegradation.

Figure 4 shows the FTIR plot of untreated PET, which has not changed significantly during week-I and II, indicated by the characteristic band of PET, exhibiting an intact matrix during the initial days of incubation. However, by the end of week- III and IV, we observe a severe drop in transmittance across the entire 1500 – 400 cm^{-1} wave number region and the peak at 1715 cm^{-1}.

The aliphatic C-H stretching in the regions between 2916 cm^{-1} and 2848 cm^{-1} observed at weeks-I and II in Fig. 4, diminishes significantly as the biodegradation reaches week-III and IV. As bacterial activity alters the PET surface, the spatial orientation of the backbone responsible for the sharp C-H stretching peaks gradually disappears over longer durations, i.e., beyond two weeks, causing the signals to smoothen towards the baseline. This also indicates the systematic loss of methylene groups due to

biodegradation. The observed shift in the carbonyl (C = O) peak at 1715 cm-1 is accompanied by a significant decrease in transmittance. This indicates possible chain scission of the PET backbone.

The major shifts in peaks in the wave numbers range 1800 cm^{-1} and 500 cm^{-1} in Fig. 4 indicate that major structural changes have occurred during weeks-III and IV. These include C = C stretching and -CH_2 bending peaks at 1500 – 1400 cm^{-1}, suggesting strong vibrational modes in the backbone benzene ring of the polymer. This indicates that the biodegradation begins to affect the structural integrity of PET. The new sharp peaks at 1340 cm^{-1} and 1240 cm^{-1} in Fig. 4 indicate strong transmittance signals from O-CH_2 vibrations, which might further affect ester bonds in the PET backbone. From Fig. 4, we see that the wave numbers ranging from 1250 – 1000 cm^{-1} contain peaks deviating significantly from the baseline in weeks-III and IV, indicating structural changes to the polymer backbone due to C-O-C asymmetric stretching and C-O ester stretching. These peaks indicate events such as ester bond cleavage, hydrolysis and further biodegradation of PET polymer, which is in accordance with the SEM image shown in Fig. 2(c), where the polymer structure begins to degrade by flaking. An analysis of the FTIR spectra in Fig. 4 also indicates a major and a minor peak between the wave numbers 900 – 700 cm^{-1}, which resulted from aromatic C-H out of plane bending vibrations. This shows that the terephthalate aromatic ring is affected due to biodegradation, which is an integral part of the polymer backbone, thus resulting in structural disassociation. Another short transmittance peak developed during week-III and IV in the wave numbers ranging from 500 cm^{-1} to 400 cm^{-1} indicates the skeletal ring deformations, which also affect the PET backbone. The lower wave numbers indicate progressive changes in the PET sample that cause loss of structural integrity beyond two weeks of biodegradation using *P. fluorescens*.

In Fig. 5, we show the FTIR spectra of the UV pretreated PET sample subjected to biodegradation. Similar to the FTIR spectra of the untreated PET sample shown in Fig. 4, we observe the diminishing peaks in the wavenumber region 2950 cm^{-1} and 2850 cm^{-1}, during weeks-II, III and IV. This indicates the reduced transmittance due to C-H stretching from week-II in UV pretreated samples, which could only be observed after week-III in the untreated samples (Fig. 4). Other significant peaks at 1715 cm^{-1} (carbonyl bond peak (C = O)), between 1500 – 1400 cm^{-1} (C = C stretching and -CH_2 bending peaks), between 1340 – 1240 cm^{-1} (O-CH_2 vibrations), and between 1250 – 1000 cm^{-1} (C-O-C asymmetric stretching, C-O ester stretching) in Fig. 5 for UV pretreated PET samples are similar to that of untreated PET samples shown in Fig. 4. However, in Fig. 4, the peaks are less prominent, whereas in the UV pretreated sample, these peaks are significant and are visible after week-II (in Fig. 5). This data is in also in concurrence with the gravimetric analysis shown in Table 1. A comparison of the FTIR spectra in Figs. 4 and 5 shows lower transmittance values in the UV pretreated samples than in the untreated samples for the peaks between 1800 and 500 cm^{-1}. The gravimetric analysis from Table 1 shows a significant reduction in weight of the UV pretreated samples, indicating that the bond vibrations responsible for the peaks could have dissociated due to possible fragmentation, and byproducts formation could have occurred due to photo assisted oxidation. Therefore, although the peaks between 1800 cm^{-1} and 500 cm^{-1} are pronounced in the untreated samples, indicating stronger bond vibrations, the UV pretreated samples likely show

reduced transmittance or heightened vibration peaks than the untreated samples. This could result from an accelerated bond dissociation and increased fragmentation, which would explain the greater weight loss observed for the UV-pretreated samples in Table 1.

For the PS polymer, from Fig. 6, we see that the control sample and early weeks-I and II samples maintained the characteristic bands of the original PS polymer. It can be observed in the aromatic C-H stretching region near 3000 cm^{-1} and the fingerprint region between 1600–1700 cm^{-1}, that the polymer structure remained largely intact during the initial stages of incubation with *P. fluorescens.* As the degradation period progressed, the spectra began to show subtle, but noticeable broadening and intensity changes, suggesting an alteration in the aromatic ring environment. These changes were evident by week-III in Fig. 6, and more pronounced by week-IV, where, the lower wavenumber region is relatively irregular, as compared to the control. A distinct sharp peak is evident from Fig. 6, for weeks-III and IV, in the wave number region ~ 700 cm^{-1}. For PS samples, the peaks in this wave number region indicate out of plane bending vibrations of the aromatic C-H bonds. This peak is not prominent in the control sample or for the samples from weeks-I and II. However, as the biodegradation progresses, more C-H aromatic vibrations are present, indicated by the sharp transmittance peak in week-III. In week-IV, this peak has slightly shortened, indicating that some of the C-H bonds could be cleaved, which is consistent with the gravimetric analysis shown in Table 1. The slight broadening around 3400 cm^{-1} wavenumber indicates the presence of an increase in hydroxyl (-OH) groups from week-I through week-IV, consistently. This indicates that more hydroxy or hydroperoxide bonds are formed, which is another indicator of the PS sample structure deterioration. The slight increase in the peaks around ~ 1500 cm^{-1} indicates that the aromatic C = C stretching vibrations are increasing over the weeks-I through IV. The weakening of C = C bonds in the aromatic rings indicates the gradual degradation of the PS samples through biodegradation. The evident broadening at around 3000 cm^{-1} aligns with PS degradation study using *Gordonia* sp. and *Novosphingobium* sp [35].

The UV pretreated PS samples shown in Fig. 7 from weeks-I to IV showed increase in the absorbed IR radiation (indicated by a decrease in transmittance) in the wavenumber region 400–800 cm^{-1}, as compared to the UV untreated PS samples. This indicates that more C-H aromatic out of plane vibrations are present in UV pretreated samples, which will result in faster biodegradation, which is in concurrence with the gravimetric analysis shown in Table 1. The absorption of IR radiation in the region 1400–1800 cm^{-1}, in Fig. 7, indicates that the aromatic C = C bond weakening is more than the UV untreated samples shown in Fig. 6. Similarly, in Fig. 7, the peak around 3400 cm^{-1} is much broader than the untreated PS sample shown in Fig. 6, which indicates that the hydroxyl or hydroperoxide bond vibrations are significantly higher than the control sample for UV pretreated samples, than that for the untreated samples.

Therefore, it could be concluded from FTIR analysis that, for PS samples, the cleaving of hydroxide/ hydroperoxide bonds could be the significant contributing factor for the additional biodegradation of UV pretreated samples, followed by the C = C bond and C-H bond cleavage.

Conclusion

In this study, the biodegradation of two different polymers (1) PS and (2) PET samples by *P. fluorescens* are investigated over a four-week period. Two different polymer conditions are considered, namely (a) untreated polymers, and (b) UV pretreated polymers for 100 hours. The samples showed progressive biodegradation, as evaluated by gravimetric analysis, SEM micrographs, and FTIR transmittance plots, using the vadose zone bacteria. The gravimetric analysis confirmed accelerated biodegradation of UV pretreated samples, for both PET and PS. For PET, the UV pretreated samples showed a weight loss of 7.11% over a four-week period (vs. 5.33% for untreated PET). Further, it was observed that the UV pretreatment resulted in an accelerated biodegradation of the sample by a week as compared to the untreated sample. For PS sample, the UV pretreatment resulted in 41.43% loss in the sample weight (vs. 32.5% for untreated PS) by the end of four weeks. SEM micrographs revealed bacteria mediated surface pitting to extensive fracturing and rugged topography in both the untreated and UV pretreated PET samples, while in PS samples, hollowing out of the layers and cavity formation was observed. The PS samples have shown more pronounced photooxidation due to UV pretreatment. A volumetric cavitation and material loss due to its porosity was observed in PS, while PET showed surface delamination and intense grooving. UV treatment accelerated cracking, which could be due to enhanced *P. fluorescens* attachment and colonization, leading to accelerated depolymerization. FTIR studies revealed that UV pretreated PET samples degradation was pronounced in the weeks-II, III and IV as compared to the biodegradation of untreated samples which progressed only during weeks-III and IV. The significant shift in the peaks in the higher wave numbers (~ 3000 cm^{-1}) towards the baseline showed a decrease in the systemic loss of methylene groups due to biodegradation. Major peak changes in transmittance were observed for both UV pretreated and untreated samples between wave numbers 1800 – 500 cm^{-1} indicating a multitude of changes in molecular vibration, which affect the backbone of the sample and result in fragmentation. Similarly, for the PS samples, the biodegradation proceeded through continuous surface alteration via hydroxyl/hydroperoxide accumulation (3400 cm^{-1}), followed by out of plane bending C-H linkages during the third and the fourth weeks, which are the major phenomena resulting in depolymerization. Gravimetric analysis provided evidence for the molecular phenomena observed using the FTIR spectra, while SEM images confirmed the micrographic evidence of the biodegradation processes. These findings reveal an integrative molecular and micrographic approach to biocatalytically driven depolymerization of PET and PS matrices using *P. fluorescens*, a plant growth promoting rhizobacterium. This shows successful biodegradation possibilities using naturally occurring bacterial strain in the vadose zone which will have implications in sustainable plastic waste valorization across various geospatial conditions, such as agriculture, Municipal Solid Waste Landfill and in improving soil health.

Declarations

Conflicts of interest

The authors declare no competing interests.

Ethical declaration

Not applicable

Author Contribution

NM conducted experimental investigation, collected the data and wrote the initial manuscript draft. MA and BS contributed to the framework analysis and structuring of the paper. DP and AAM supported in image analysis and preparation. SA provided supervision, modification, critical revision and finalized the manuscript draft. All authors have read and approved the final manuscript and have no competing interests to declare

Acknowledgement

The authors would like to acknowledge the grants NITC/R&C/FRGPhaseIV/2023-24 and ANRF/ECRG/2025/004526/ENS for the support during this study.

Data availability statement

The data used in this study can be found in the manuscript, visually in the form of images.

References

1. Chand SK, Yatirajula SK, Dalai A, Singh S, Boorla V, Singh S, et al. Strategic pathways for sustainable plastic management through a circular economy approach in India. Discover Sustain. 2025;6(1):20. https://doi.org/10.1007/s43621-025-02218-1.
2. Thompson RC, Moore CJ, Vom Saal FS, Swan SH. Plastics, the environment and human health: current consensus and future trends. Phil Trans R Soc B. 2009;364(1526):2153–66. https://doi.org/10.1098/rstb.2009.0053.
3. Oehlmann J, Schulte-Oehlmann U, Kloas W, Jagnytsch O, Lutz I, Kusk KO, et al. A critical analysis of the biological impacts of plasticizers on wildlife. Phil Trans R Soc B. 2009;364(1526):2047–62. https://doi.org/10.1098/rstb.2008.0242.
4. Wright SL, Kelly FJ. Plastic and human health: a micro issue? Environ Sci Technol. 2017;51(12):6634–47. https://doi.org/10.1021/acs.est.7b00423.
5. Raj M, Ghosh A, Ilame T, Kumar S. Plastic waste management strategies: planning through sustainable lens and way forward towards circular economy. Discover Sustain. 2025;6:361.

https://doi.org/10.1007/s43621-025-01103-1.

6. Ragaert K, Delva L, Van Geem K. Mechanical and chemical recycling of solid plastic waste. Waste Manage. 2017;69:24–58. https://doi.org/10.1016/j.wasman.2017.07.044.
7. Nagy Á, Kuti R. The environmental impact of plastic waste incineration. AARMS. 2016;15(3):231–7. https://doi.org/10.32565/aarms.2016.3.3.
8. Maurya P, Kumar R. Emerging threat of microplastics across environmental matrices encompassing sources ecotoxicological effects and management strategies within the framework of Sustainable Development Goals (SDGs). Discover Sustain. 2026;7:42. https://doi.org/10.1007/s43621-025-02510-0.
9. Mutshekwa T, Motitsoe SN, Maiyana VP, Mofu L, Ajay K, Phophi L. Microplastic occurrence and densities in small subtropical reservoirs of Southern Africa. Discover Sustain. 2025;6:132. https://doi.org/10.1007/s43621-025-00928-0.
10. Dalu T, Themba ST, Dondofema F, Wu N, Munyai LF. Assessing microplastic abundances in freshwater fishes in a subtropical African reservoir. Discover Sustain. 2024;5:360. https://doi.org/10.1007/s43621-024-00589-5.
11. Zhang J, Ren S, Xu W, Liang C, Li J, Zhang H, et al. Effects of plastic residues and microplastics on soil ecosystems: A global meta-analysis. J Hazard Mater. 2022;435:129065. https://doi.org/10.1016/j.jhazmat.2022.129065.
12. Weithmann N, Möller JN, Löder MGJ, Piehl S, Laforsch C, Freitag R. Organic fertilizer as a vehicle for the entry of microplastic into the environment. Sci Adv. 2018;4(4):eaap8060. https://doi.org/10.1126/sciadv.aap8060.
13. Li C, Chen J, Wang J, Han P, Luan Y, Ma X, et al. Phthalate esters in soil, plastic film, and vegetable from greenhouse vegetable production bases in Beijing, China: concentrations, sources, and risk assessment. Sci Total Environ. 2016;568:1037–43. https://doi.org/10.1016/j.scitotenv.2016.06.077.
14. Browne MA, Crump P, Niven SJ, Teuten E, Tonkin A, Galloway T, et al. Accumulation of microplastic on shorelines worldwide: sources and sinks. Environ Sci Technol. 2011;45(11):9175–9. https://doi.org/10.1021/es201811s.
15. Dalu T, Xozumti AP, Dalu MT, Munyai LF, Nkosi SM, Themba ST, et al. Microplastics in municipal water: analysing variations in contamination in a Lowveld city, South Africa. Discover Sustain. 2025;6:850. https://doi.org/10.1007/s43621-025-01690-z.
16. Sunitha T, Monisha V, Sivanesan S, Vasanthy M, Prabhakaran M, Omine K, et al. Micro-plastic pollution along the Bay of Bengal coastal stretch of Tamil Nadu, South India. Sci Total Environ. 2021;756:144073. https://doi.org/10.1016/j.scitotenv.2020.144073.
17. Karwadiya J, Kerketta AR, Pathak SK, Srivastava S, Darbha GK. Agronomic practices and road proximity drive plastic pollution in agricultural soils: Insights from Bihar, India on weathering, elemental association, and ecological risk. Environ Pollut. 2025;365:126975. https://doi.org/10.1016/j.envpol.2025.126975.

18. Mahreen L, C A, Warrier AK. Baseline assessment of microplastic contamination in agricultural soils from the coastal stretches of Karnataka and Goa, Southwestern India. Environ Monit Assess. 2025;197(11):1053. https://doi.org/10.1007/s10661-025-14513-5.
19. Tziourrou P, Golia EE. Plastics in agricultural and urban soils: interactions with plants, micro-organisms, inorganic and organic pollutants: an overview of polyethylene (PE) litter. Soil Syst. 2024;8(1):23. https://doi.org/10.3390/soilsystems8010023.
20. Kumari A, Chakraborty S. Vertical profiling of microplastics in agricultural soils: polymer types, metal interactions, and implication on crop rooting zones. Environ Monit Assess. 2026;198:291. https://doi.org/10.1007/s10661-026-15148-w.
21. Al Mamun A, Prasetya TAE, Dewi IR, Ahmad M. Microplastics in human food chains: Food becoming a threat to health safety. Sci Total Environ. 2023;858(Pt 3):159834. https://doi.org/10.1016/j.scitotenv.2022.159834.
22. Jerie S, Chireshe A, Shabani T, Shabani T, Maswoswere P, Mudyazhezha OC, et al. Environmental impacts of plastic waste management practices in urban suburbs areas of Zimbabwe. Discover Sustain. 2024;5:435. https://doi.org/10.1007/s43621-024-00588-6.
23. Jun SR, Wassenaar TM, Nookaew I, Hauser L, Wanchai V, Land M, et al. Diversity of Pseudomonas genomes, including Populus-associated isolates, as revealed by comparative genome analysis. Appl Environ Microbiol. 2016;82(2):375–83. https://doi.org/10.1128/AEM.02612-15.
24. Garrido-Sanz D, Meier-Kolthoff JP, Göker M, Martín M, Rivilla R, Redondo-Nieto M. Genomic and genetic diversity within the Pseudomonas fluorescens complex. PLoS ONE. 2016;11(2):e0150183. https://doi.org/10.1371/journal.pone.0150183.
25. Dhaka V, Singh S, Ramamurthy PC, Samuel J, Swamy Sunil Kumar Naik T, Khasnabis S, et al. Biological degradation of polyethylene terephthalate by bacteria. Environ Sci Pollut Res. 2023;30(49):116488–97. https://doi.org/10.1007/s11356-022-20324-9.
26. Zhu Y, Wang H, Bai J, Qi Y, Han D. Biodegradation potential of Gordonia spp. on polypropylene and polystyrene: enhanced degradation through pretreatment. Front Microbiol. 2025;16:1621498. https://doi.org/10.3389/fmicb.2025.1621498.
27. Santhosh S, Narenkumar J, Vadakkan K, Nandini M, Rajasekar A, Rajamohan R. Enterobacter hormaechei mediated biodegradation of PET: a sustainable approach to plastic waste. Biodegradation. 2025;36:88. https://doi.org/10.1007/s10532-025-10183-9.
28. Wang J, Liu R, Zhao S, Zhang B, Shao Z. Construction of an efficient polystyrene-degrading microbial consortium based on degrading and non-degrading bacteria predominant in biofilms of marine plastic debris. Front Mar Sci. 2025;12:1569583. https://doi.org/10.3389/fmars.2025.1569583.
29. Montazer Z, Habibi-Najafi MB, Mohebbi M, Oromiehei A. Microbial degradation of UV-pretreated low-density polyethylene films by novel polyethylene-degrading bacteria isolated from plastic-dump soil. J Polym Environ. 2018;26(9):3613–25. https://doi.org/10.1007/s10924-018-1245-0.
30. Walters I, Turner A. Degradation of polyethylene terephthalate bottle fragments in the rhizob environment: An empirical study of structural and chemical changes. Environ Pollut.

2026;366:127885. https://doi.org/10.1016/j.envpol.2026.127885.

31. Adithama RM, Munifah I, Yanto DHY, Meryandini A. Biodegradation of low-density polyethylene microplastic by new halotolerant bacteria isolated from saline mud in Bledug Kuwu, Indonesia. Bioresour Technol Rep. 2023;22:101466. https://doi.org/10.1016/j.biteb.2023.101466.
32. Chaudhary AK, Chaitanya K, Vijayakumar R. Synergistic effect of UV and chemical treatment on biological degradation of Polystyrene by Cephalosporium strain NCIM 1251. Arch Microbiol. 2021;203(5):2183–91. https://doi.org/10.1007/s00203-021-02228-3.
33. Sepperumal U, Markandan M, Natarajan A. Electron microscopic studies of Polyethylene terephthalate degradation potential of Pseudomonas species. J Microbiol Biotechnol Res. 2013;3(4):104–10.
34. Cada EJG, Muyot MLC, Sison JMC, Baculi RQ. Enhanced in vitro biodegradation of low-density polyethylene using alkaliphilic bacterial consortium supplemented with iron oxide nanoparticles. Philipp Sci Lett. 2019;12(1):55–69.
35. Liu R, Zhao S, Zhang B, Li G, Fu X, Yan P, et al. Biodegradation of polystyrene (PS) by marine bacteria in mangrove ecosystem. J Hazard Mater. 2023;442:130056. https://doi.org/10.1016/j.jhazmat.2022.130056.

Figures

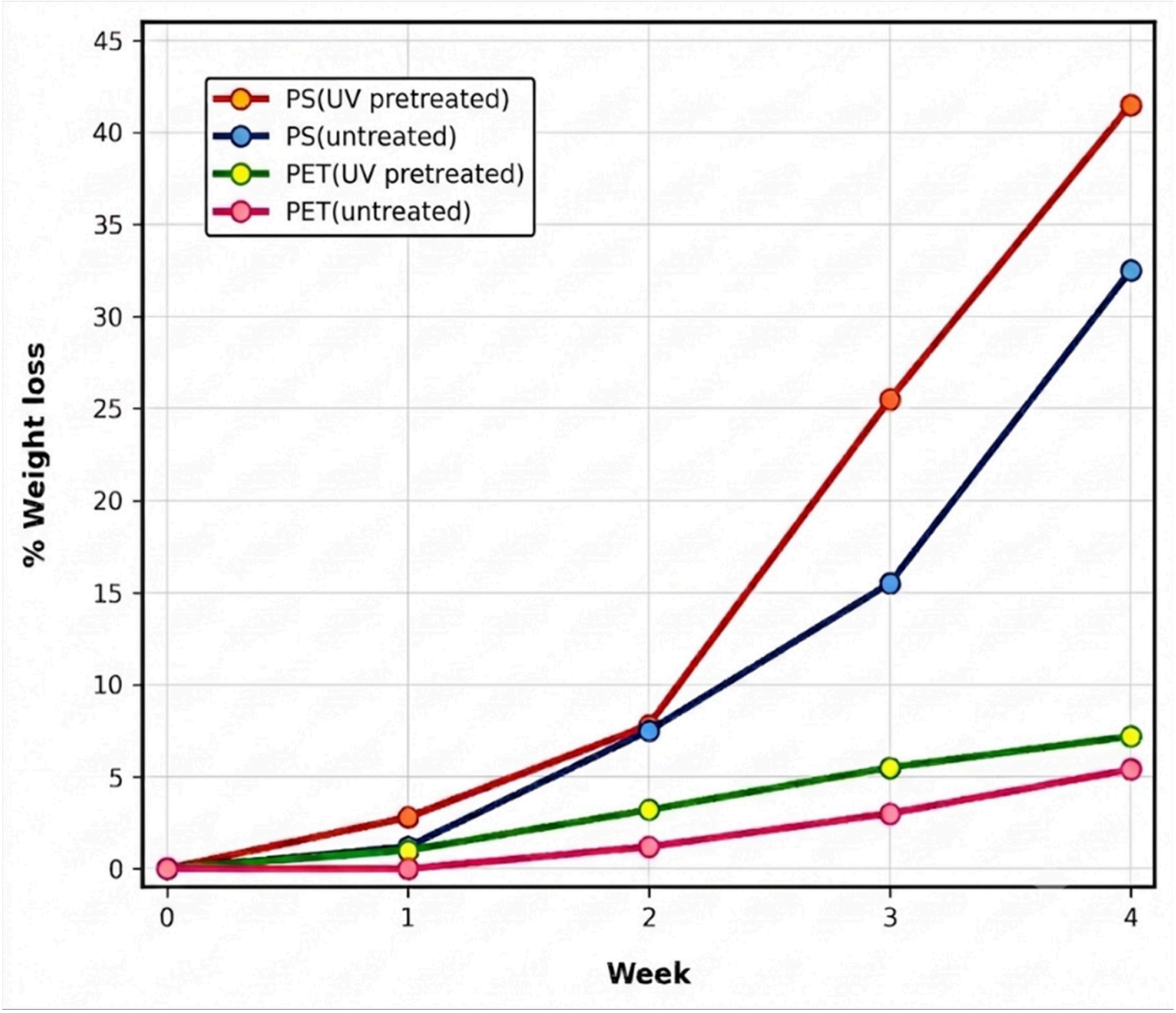


Figure 1

Weight loss in the samples over four weeks due to biodegradation

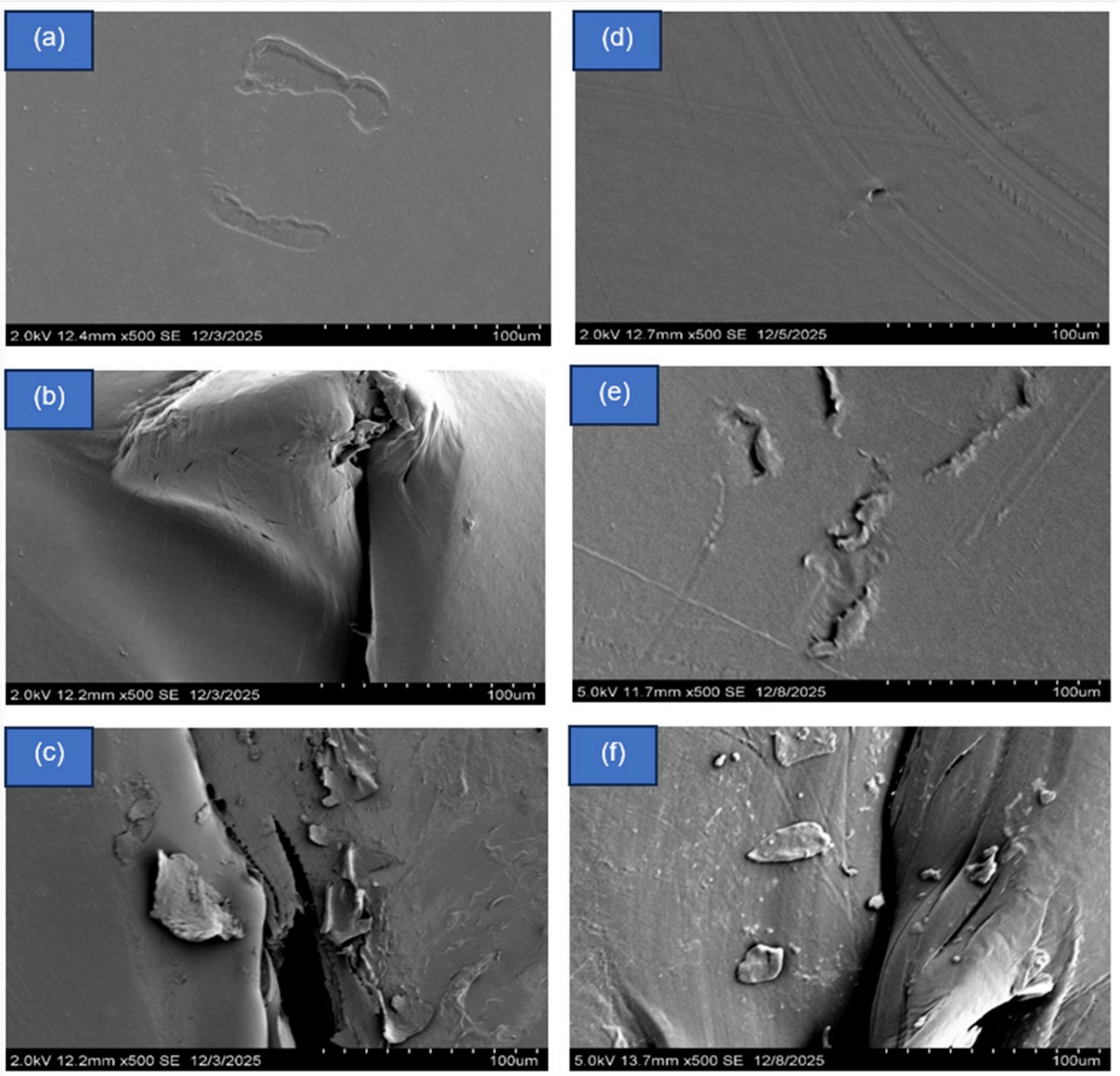


Figure 2

Scanning electron micrographs of PET - (a) Untreated control PET, (b) week-II untreated PET, (c) week-IV untreated PET, (d) UV pretreated control PET, (e) week-II UV pretreated PET, (f) week-IV UV pretreated PET

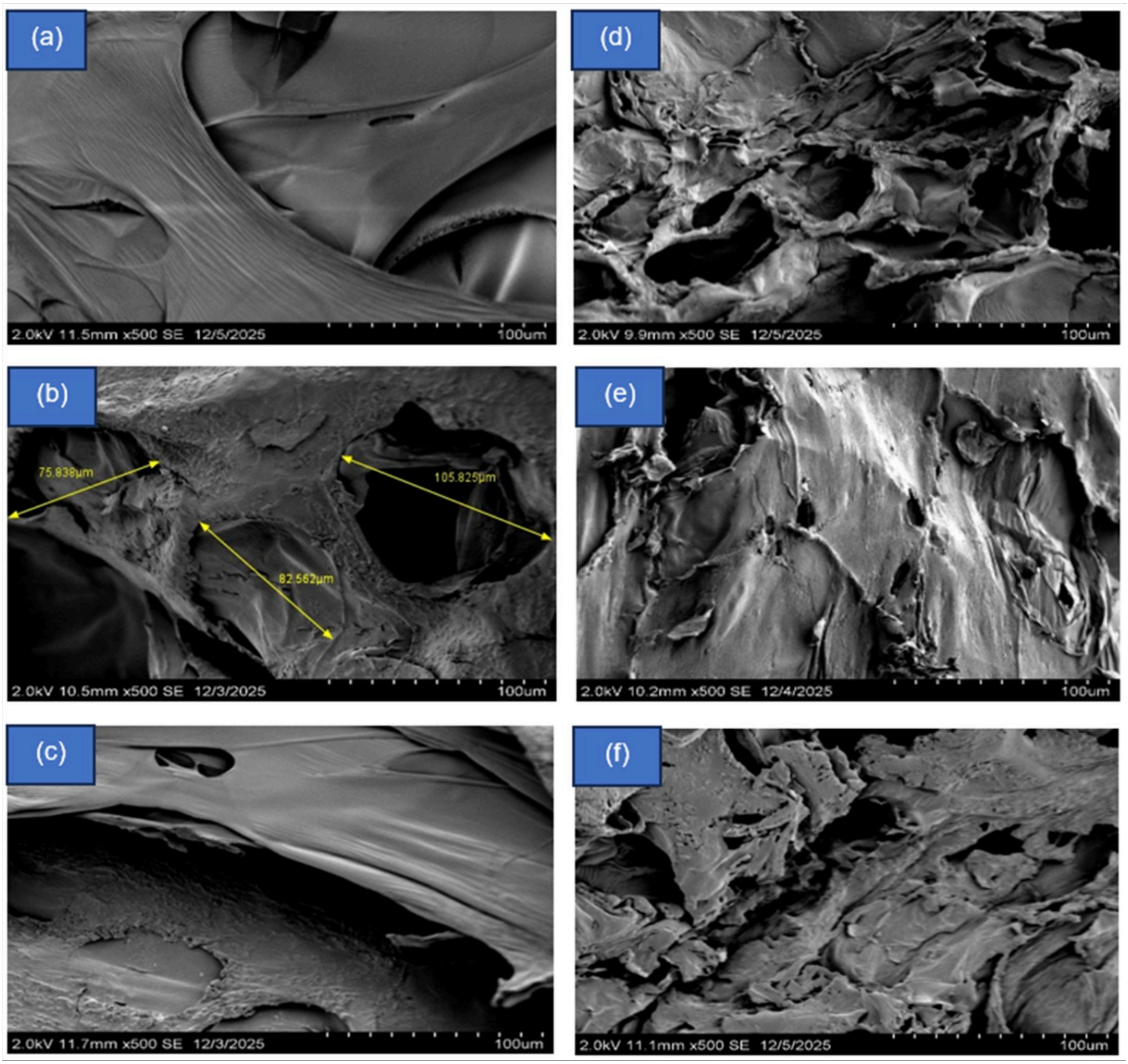


Figure 3

Scanning electron micrographs of PS. After pretreatment, the surface morphology of PS changed significantly. (a) Untreated control PS, (b) week-II untreated PS exhibiting localized cavities and microgrooves with lateral dimensions measured at 75.838 µm, 82.562 µm, and 105.825 µm, (c) week-IV untreated PS, (d) UV pretreated control PS, (e) week-II UV pretreated PS, (f) week-IV UV pretreated PS

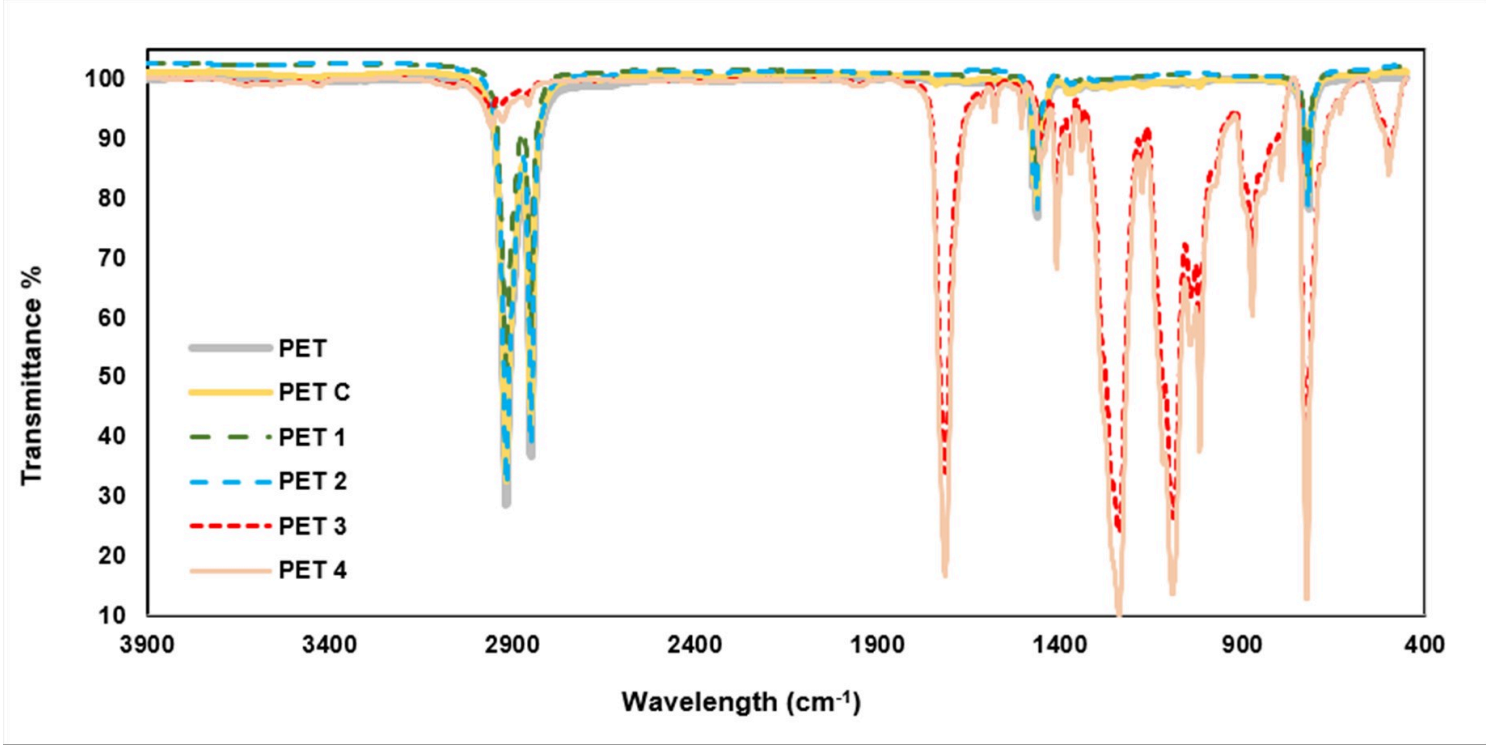


Figure 4

ATR-FTIR analysis of untreated PET biodegradation pattern by P. fluorescens. The control sample is indicated as PET C, and the PET biodegraded samples from week-I, II, III, IV are represented as PET 1, PET 2, PET 3, PET 4, respectively. A comparison with the PET sample placed in air for four weeks is also presented, labelled as PET

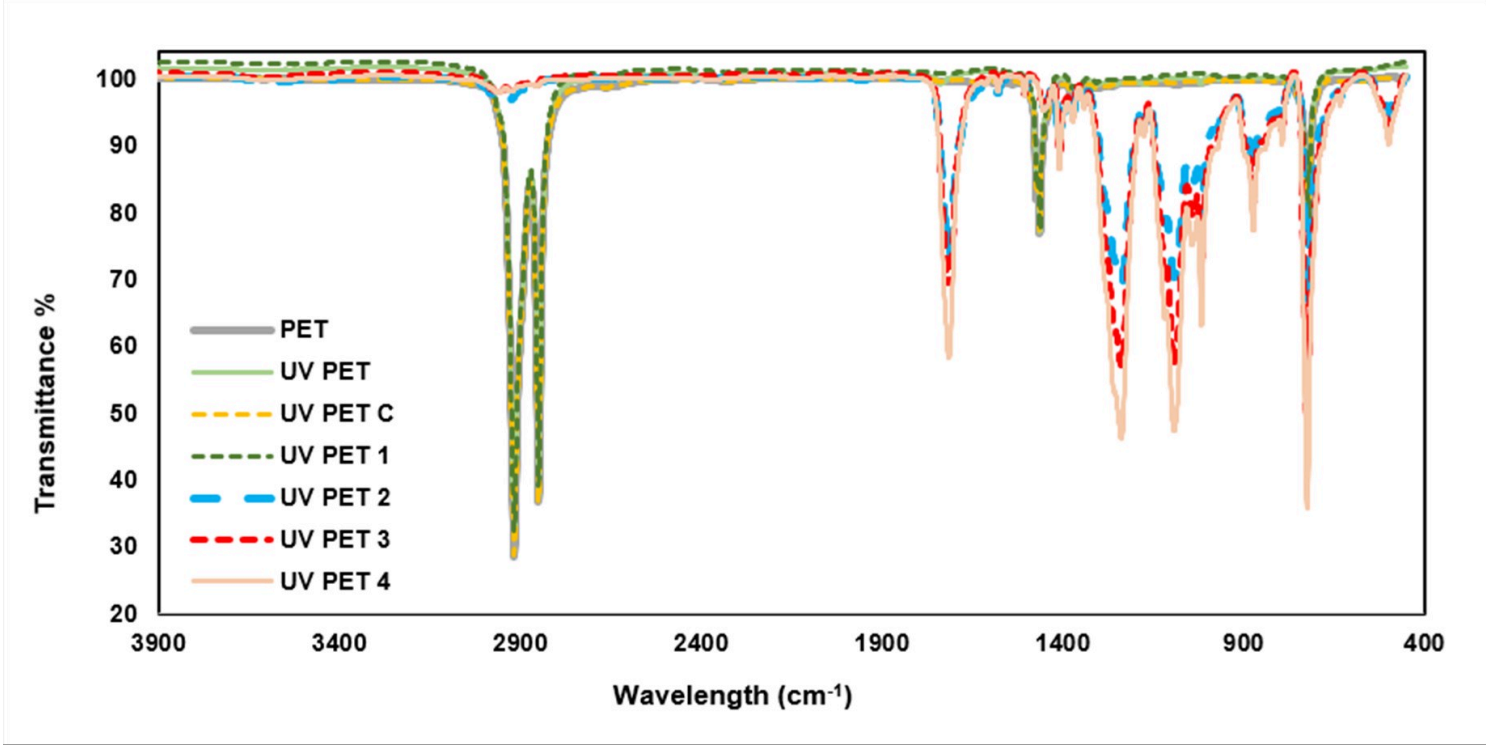


Figure 5

ATR-FTIR analysis of UV pretreated PET biodegradation pattern by P. fluorescens. The control sample is indicated as UV PET C, and the PET biodegraded samples from week-I, II, III, IV are represented as UV PET 1, UV PET 2, UV PET 3, UV PET 4, respectively. Additionally, comparisons with a PET sample (PET) and a UV pretreated PET sample (UV PET), both placed in air for four weeks, are presented

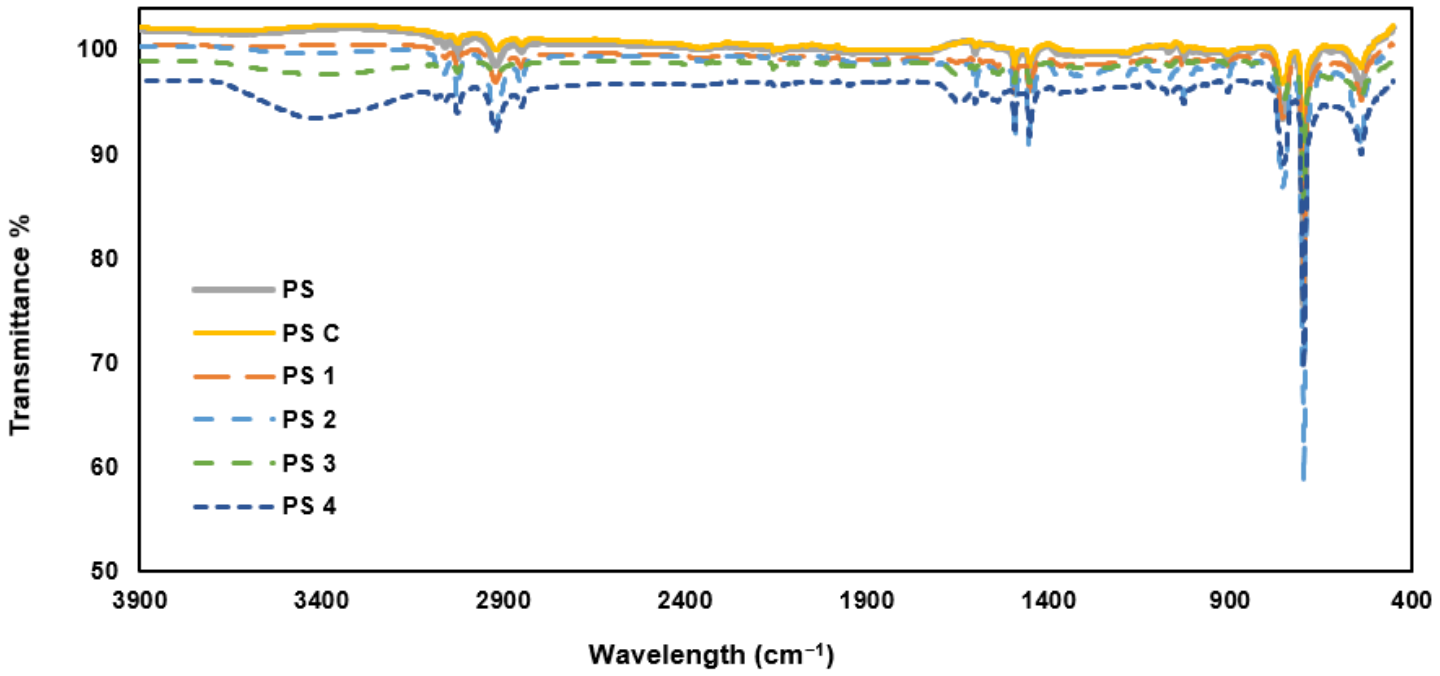


Figure 6

ATR-FTIR analysis of untreated PS biodegradation pattern by P. fluorescens. The control sample is indicated as PS C, and the PS biodegraded samples from week-I, II, III, IV are represented as PS 1, PS 2, PS 3, PS 4, respectively. A comparison with a PS sample placed in air for four weeks is also presented, labelled as PS

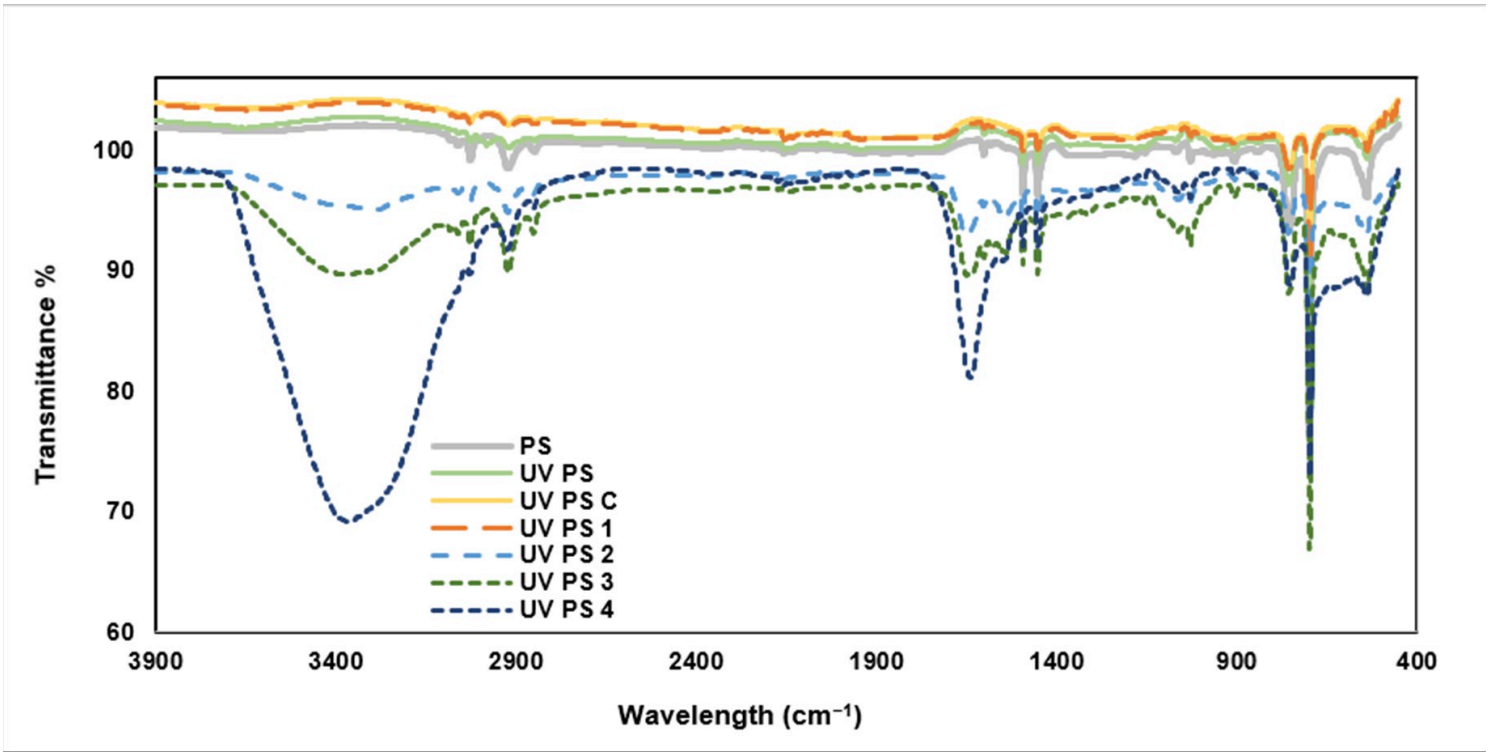


Figure 7

ATR-FTIR analysis of UV treated PS biodegradation pattern by P. fluorescens. The control sample is indicated as UV PS C, and the PS biodegraded samples from week-I, II, III, IV are represented as UV PS 1, UV PS 2, UV PS 3, UV PS 4, respectively. Additionally, comparisons with a PS sample (PS) and a UV pretreated PS sample (UV PS), both placed in air for four weeks, are presented